J. Mex. Chem. Soc. **2025**, *69*(2)
Regular Issue

ISSN-e 2594-0317

Microwave-Assisted Synthesis and Evaluation of the Optoelectronic Properties of Metallated *Meso*-Tetraphenylporphyrin Complex

Rosalio Velarde-Barraza, Edgar A. Reynoso-Soto, Ignacio A. Rivero*

Tecnológico Nacional de México/Instituto Tecnológico de Tijuana, Centro de Graduados e Investigación en Química, Blvd. Alberto Limón Padilla S/N 22510 Tijuana, B. C., México.

***Corresponding author:** Ignacio A. Rivero, email: irivero@tectijuana.mx

Received October 20th, 2023; Accepted April 11th, 2024.

DOI for the article: http://dx.doi.org/10.29356/jmcs.v69i2.2156

Supplementary Information

J. Mex. Chem. Soc. **2025**, *69*(2)
Regular Issue

ISSN-e 2594-0317

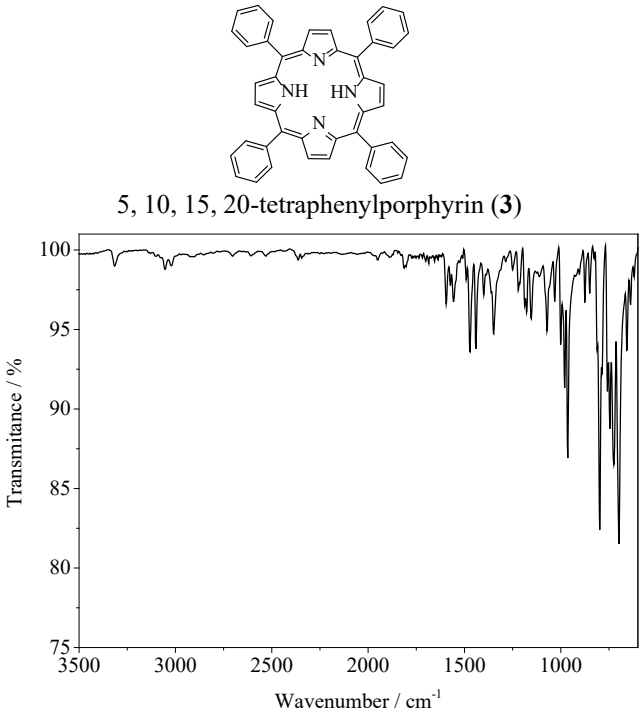

Fig. S1. FTIR spectrum of compound **3**.

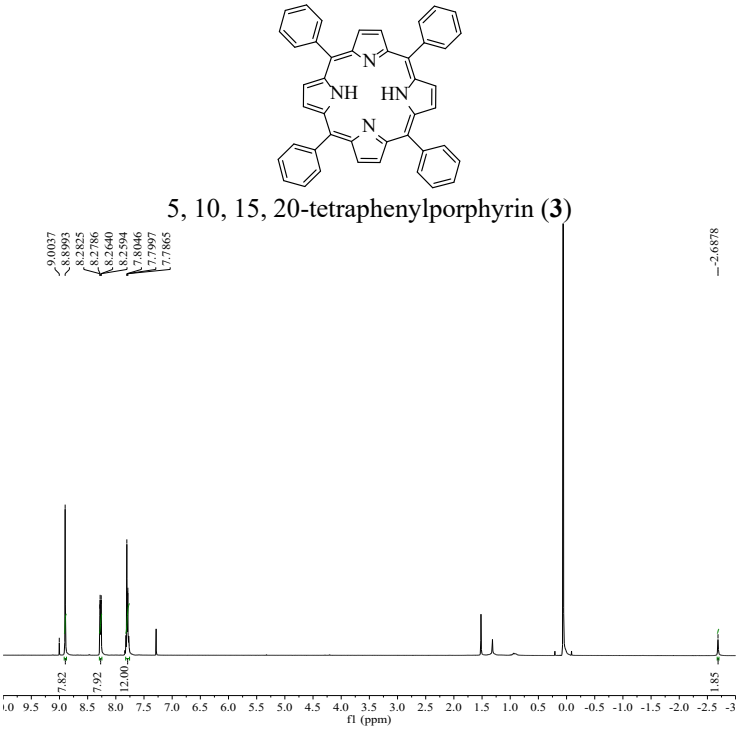

Fig. S2. ^{1}H NMR spectrum (400 MHz, $CDCl_3$) of compound **3**.

J. Mex. Chem. Soc. **2025**, *69*(2)
Regular Issue

ISSN-e 2594-0317

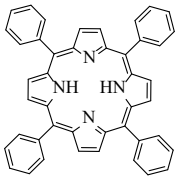

5, 10, 15, 20-tetraphenylporphyrin (**3**)

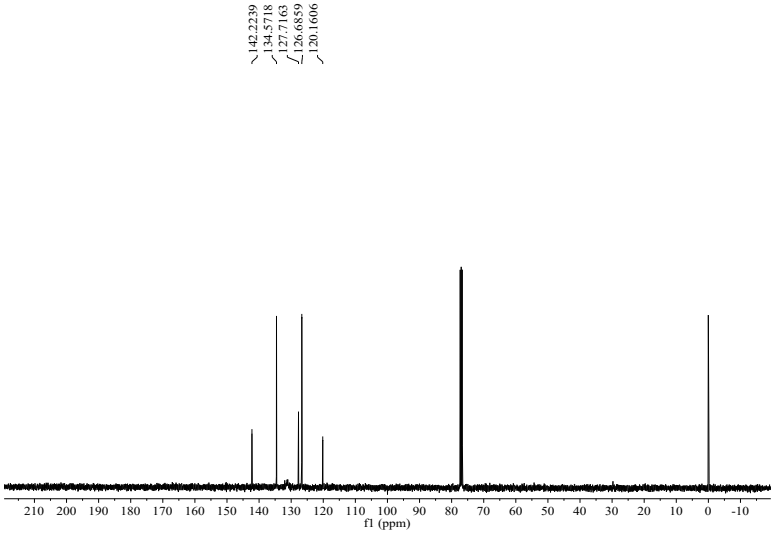

Fig. S3. ^{13}C NMR spectrum (400 MHz, $CDCl_3$) of compound **3**.

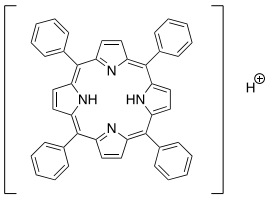

Chemical formula: $[C_{44}H_{30}N_4]H^+$
Molecular Weight: 615.0

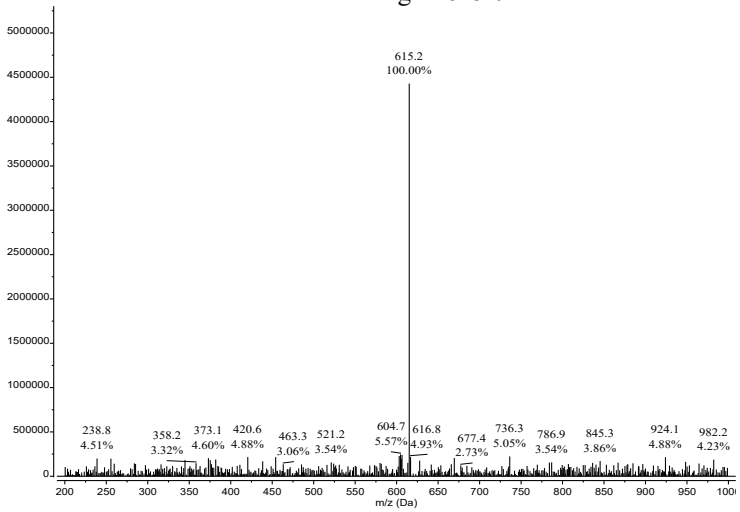

Fig. S4. Mass spectrum (ESI-MS) of compound **3**.

J. Mex. Chem. Soc. **2025**, *69*(2)
Regular Issue

ISSN-e 2594-0317

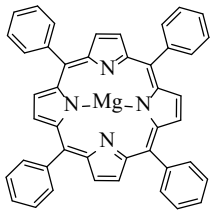

Magnesium 5, 10, 15, 20-tetraphenylporphyrin (**4a**)

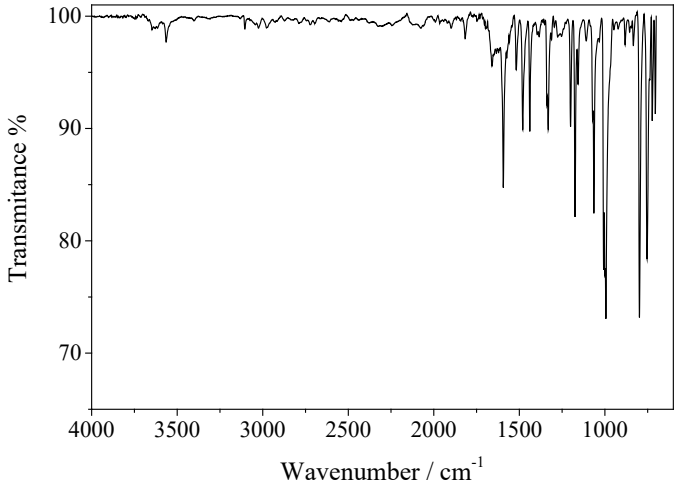

Fig. S5. FTIR spectrum of compound **4a**.

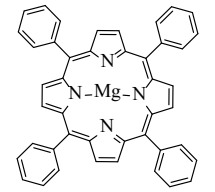

Magnesium 5, 10, 15, 20-tetraphenylporphyrin (**4a**)

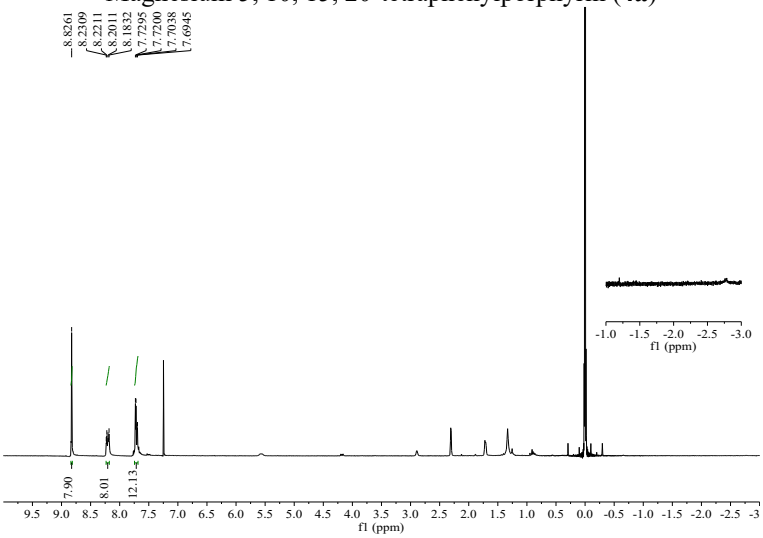

Fig. S6. ^{1}H NMR spectrum (200 MHz, $CDCl_3$) of compound **4a**.

J. Mex. Chem. Soc. **2025**, *69*(2)
Regular Issue

ISSN-e 2594-0317

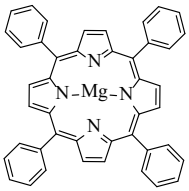

Magnesium 5, 10, 15, 20-tetraphenylporphyrin (**4a**)

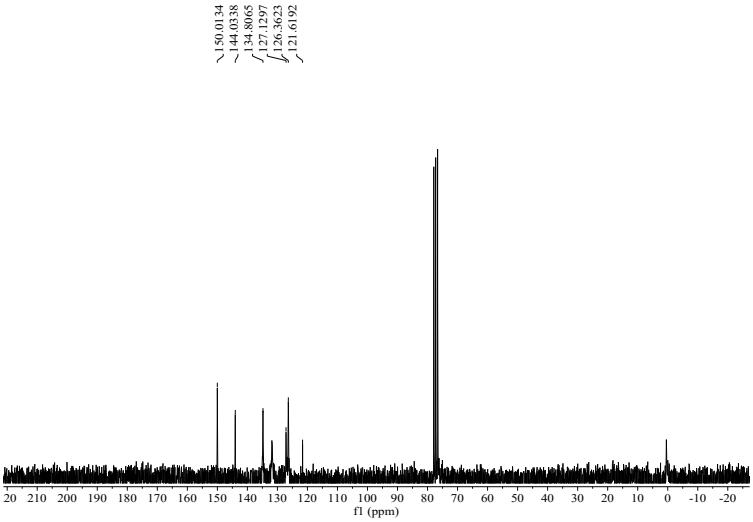

Fig. S7. ^{13}C NMR spectrum (50 MHz, $CDCl_3$) of compound **4a**.

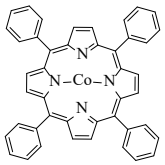

Cobalt 5, 10, 15, 20-tetraphenylporphyrin (**4b**)

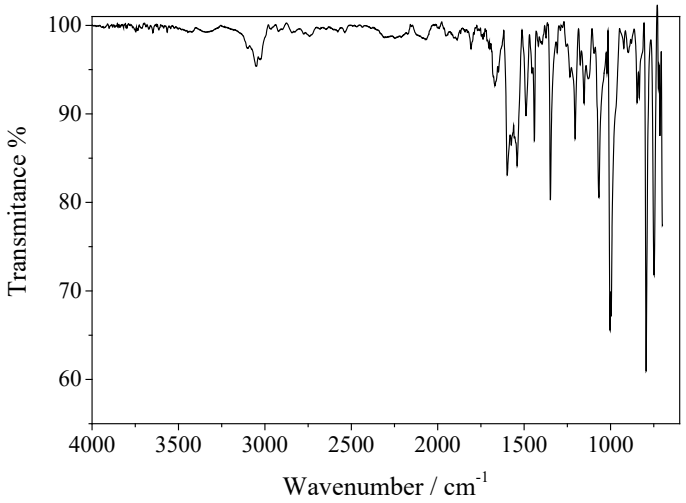

Fig. S8. FTIR spectrum of compound **4b**.

J. Mex. Chem. Soc. **2025**, *69*(2)
Regular Issue

ISSN-e 2594-0317

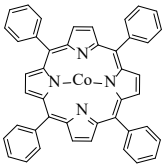

Cobalt 5, 10, 15, 20-tetraphenylporphyrin (**4b**)

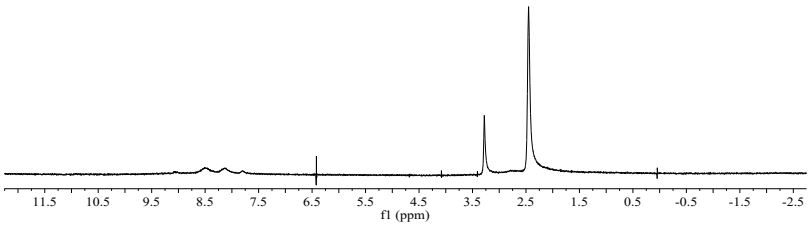

Fig. S9. ^{1}H NMR spectrum (200 MHz, $CDCl_3$) of compound **4b**.

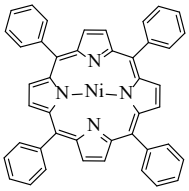

Nickel 5, 10, 15, 20-tetraphenylporphyrin (**4c**)

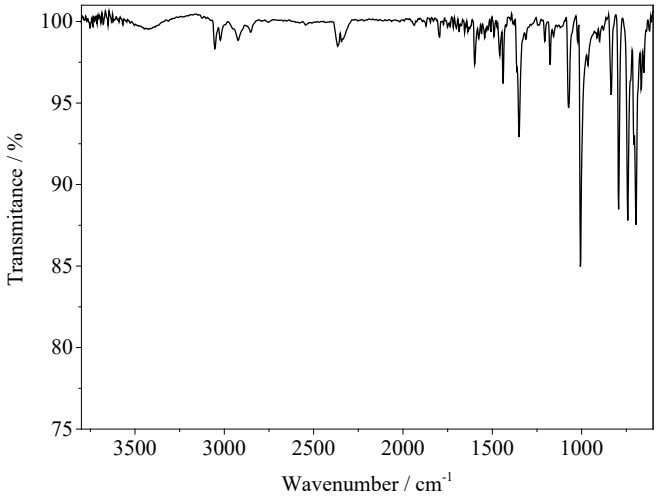

Fig. S10. FTIR spectrum of compound **4c**.

J. Mex. Chem. Soc. **2025**, *69*(2)
Regular Issue

ISSN-e 2594-0317

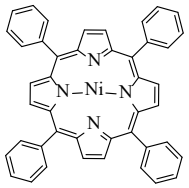

Nickel 5, 10, 15, 20-tetraphenylporphyrin (**4c**)

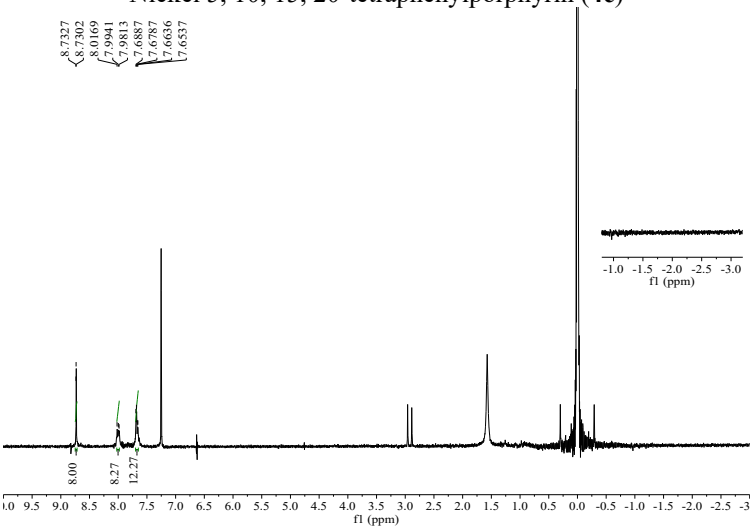

Fig. S11. ^{1}H NMR spectrum (200 MHz, $CDCl_3$) of compound **4c**.

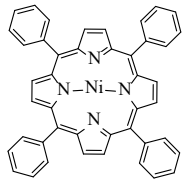

Nickel 5, 10, 15, 20-tetraphenylporphyrin (**4c**)

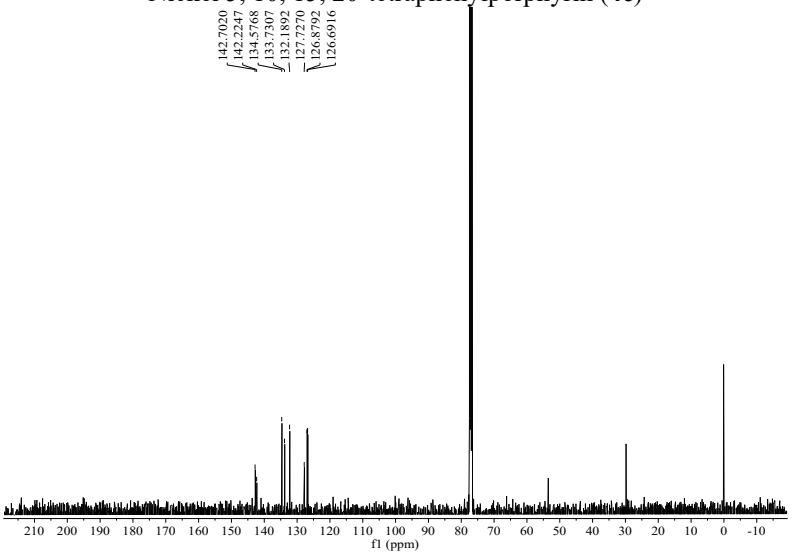

Fig. S12. ^{13}C NMR spectrum (100 MHz, $CDCl_3$) of compound **4c**.

J. Mex. Chem. Soc. **2025**, *69*(2)
Regular Issue

ISSN-e 2594-0317

Copper 5, 10, 15, 20-tetraphenylporphyrin (**4d**)

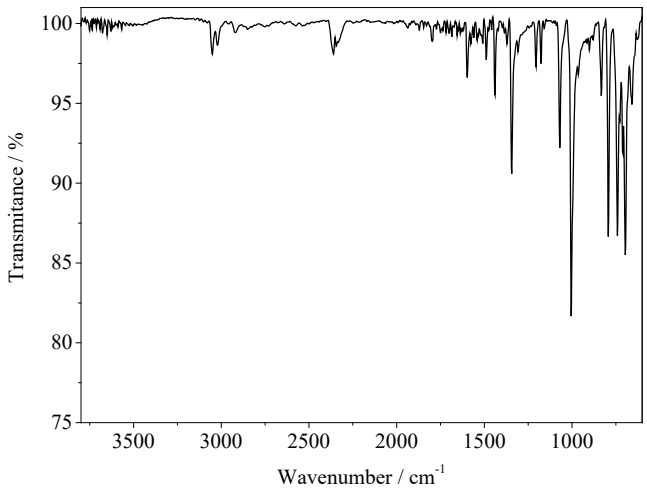

Fig. S13. FTIR spectrum of compound **4d**.

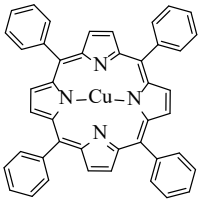

Copper 5, 10, 15, 20-tetraphenylporphyrin (**4d**)

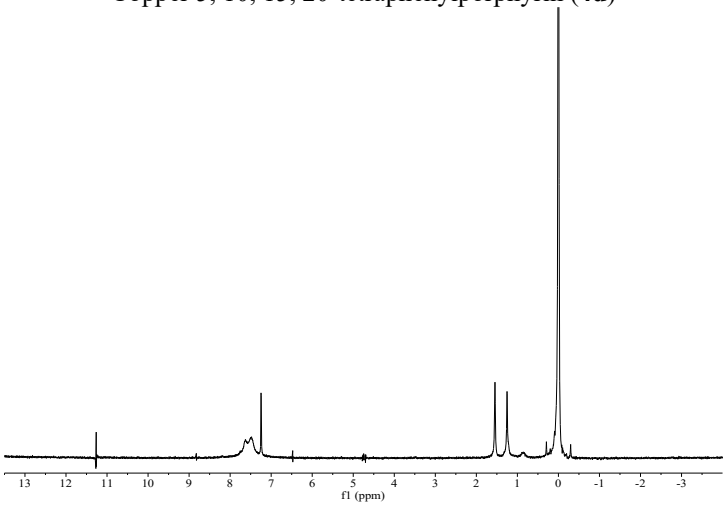

Fig. S14. ^{1}H NMR spectrum (200 MHz, $CDCl_3$) of compound **4d**.

J. Mex. Chem. Soc. **2025**, *69*(2)
Regular Issue

ISSN-e 2594-0317

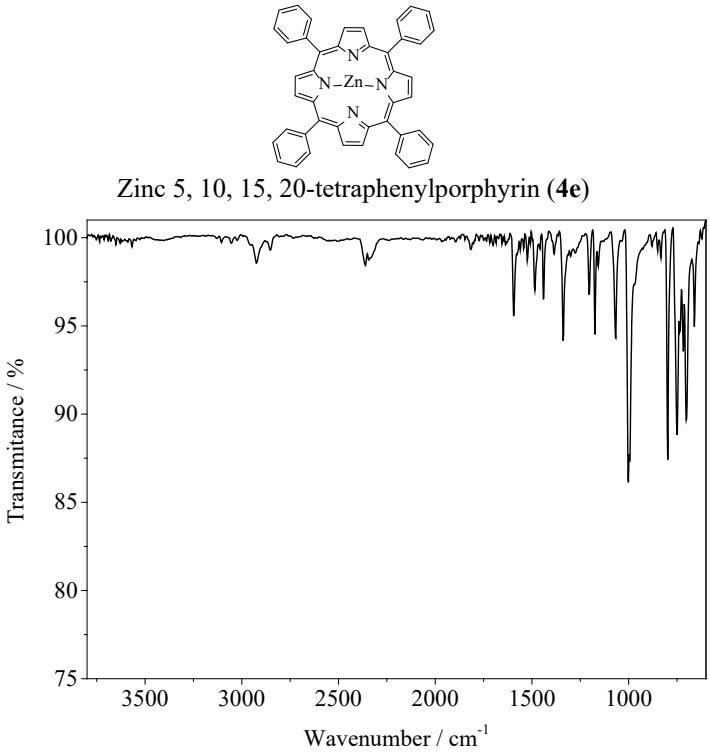

Fig. S15. FTIR spectrum of compound **4e**.

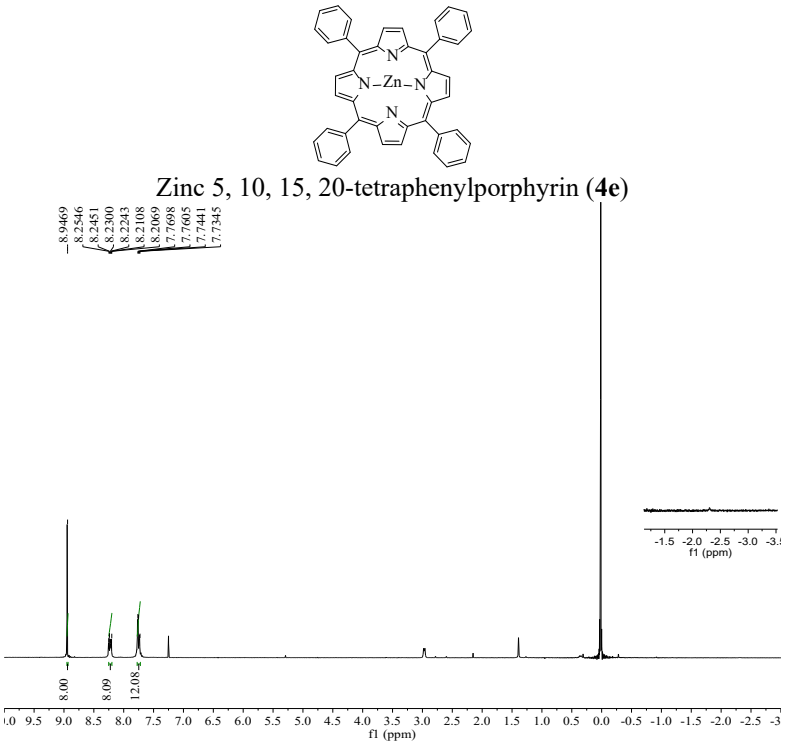

Fig. S16. ^{1}H NMR spectrum (200 MHz, $CDCl_3$) of compound **4e**.

J. Mex. Chem. Soc. **2025**, *69*(2)
Regular Issue

ISSN-e 2594-0317

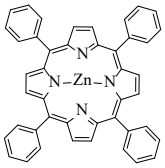

Zinc 5, 10, 15, 20-tetraphenylporphyrin (**4e**)

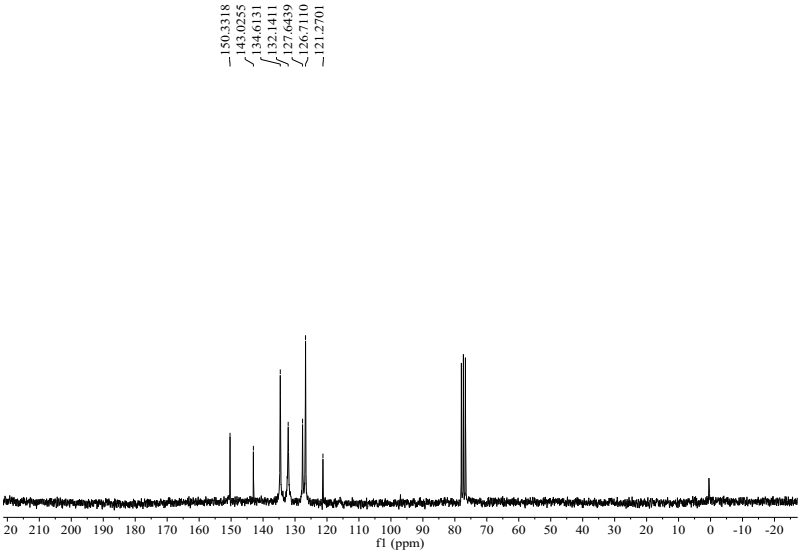

Fig. S17. ^{13}C NMR spectrum (50 MHz, $CDCl_3$) of compound **4e**.

Photophysical properties

Ultraviolet-visible absorption spectroscopy

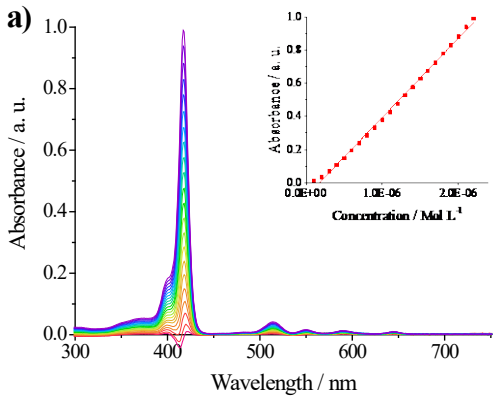

Equation	y = a + b*x
Plot	Absorbance
Weight	No Weighting
Intercept	-0.08208
Slope	476411.63185
Residual Sum of Squares	0.00535
Pearson's r	0.99867
R-Square(COD)	0.99735
Adj. R-Square	0.99721

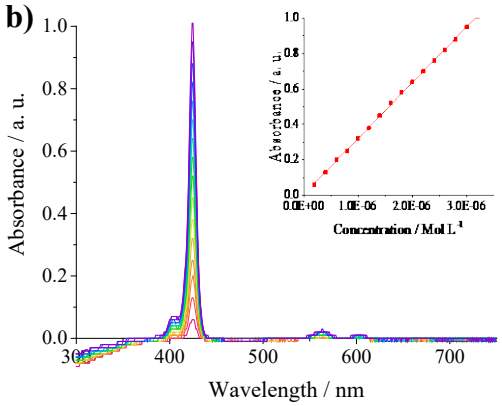

Equation	y = a + b*x
Plot	Absorbance
Weight	No Weighting
Intercept	0.00525
Slope	314926.47059
Residual Sum of Squares	4.63676E-4
Pearson's r	0.99983
R-Square(COD)	0.99966
Adj. R-Square	0.99963

J. Mex. Chem. Soc. **2025**, *69*(2)
Regular Issue

ISSN-e 2594-0317

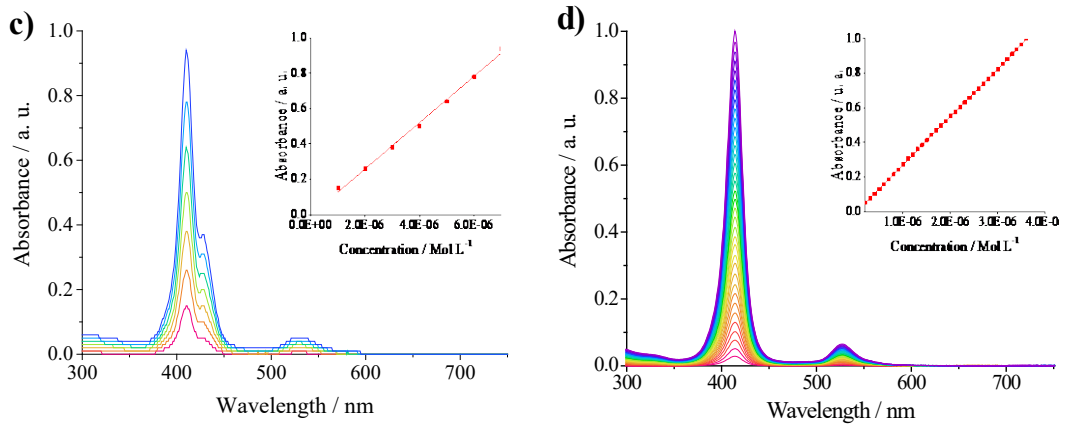

Equation	y = a + b*x
Plot	Absorbance
Weight	No Weighting
Intercept	-0.00286
Slope	131071.42857
Residual Sum of Squares	0.00185
Pearson's r	0.99808
R-Square(COD)	0.99616
Adj. R-Square	0.99539

Equation	y = a + b*x
Plot	Absorbance
Weight	No Weighting
Intercept	-0.00393
Slope	276928.95753
Residual Sum of Squares	4.12509E-4
Pearson's r	0.99993
R-Square(COD)	0.99986
Adj. R-Square	0.99986

Fig. S18. UV-vis absorption spectra of compounds **3 (a)**, **4a (b)**, **4b (c)** and **4c (d)**, in DCM.

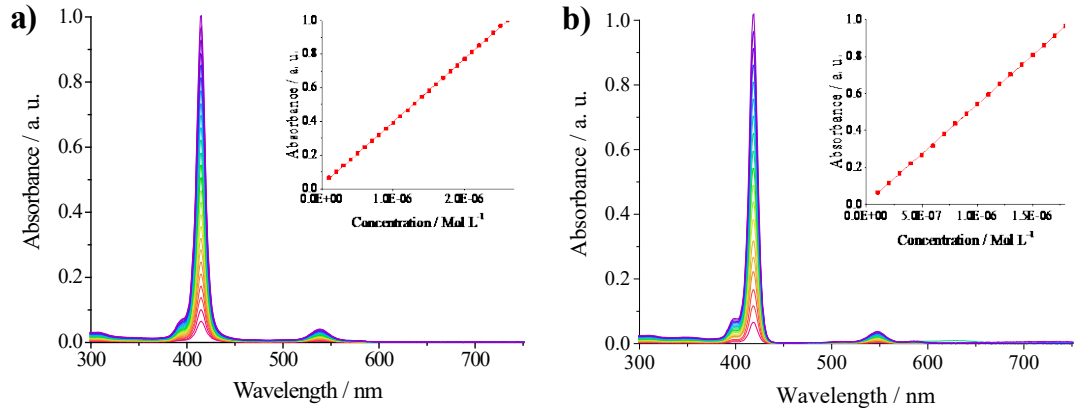

Equation	y = a + b*x
Plot	Absorbance
Weight	No Weighting
Intercept	0.02022
Slope	376637.60684
Residual Sum of Squares	3.54995E-4
Pearson's r	0.99991
R-Square(COD)	0.99983
Adj. R-Square	0.99982

Equation	y = a + b*x
Plot	Absorbance
Weight	No Weighting
Intercept	0.00788
Slope	533026.31579
Residual Sum of Squares	2.51566E-4
Pearson's r	0.99992
R-Square(COD)	0.99984
Adj. R-Square	0.99984

Fig. S19. UV-vis absorption spectra of compounds **4d (a)** and **4e (b)** in DCM.

Fluorescence emission spectroscopy

Emission spectra of the *meso*-tetraphenylporphyrin metal analogs were obtained with a Varian Eclipse spectrophotometer using a 1 cm quartz cell in a measurement range of 500-800 nm at a scan rate of 600 nm/min. Samples were solubilized in DCM to obtain a $1x10^{-4}$ M stock solution. The initial measurement

J. Mex. Chem. Soc. **2025**, *69*(2)
Regular Issue

ISSN-e 2594-0317

solution for all compounds evaluated was $1x10^{-7}$ M and then for each additional measurement aliquot additions of $1x10^{-7}$ M were made to obtain a gradual measurement of their increase with respect to concentration until a saturation of fluorescence emission was obtained. Fluorescence quantum yields were obtained by the following equation:

$$\Phi_f(\mathrm{X}) = \left(\frac{A_s}{A_x}\right)\left(\frac{F_x}{F_s}\right)\left(\frac{n_x}{n_s}\right)^2 \Phi_f(\mathrm{S})$$

Where $\Phi_f(X)$ is the fluorescence quantum yield of the sample. *A* is the absorbance at the excitation wavelength, *F* represents the area under the curve of the emission band, *n* represents the refractive index of the solvent used, *S* is the standard compound used and *X* is the sample to be evaluated. [1,2]

Computational study

Table S1. Calculated electronic excitation energies, oscillator strength and electronic transition.

Compound	λ_{exi} (nm)	*E* (eV)	*f*	Transition	*P*
3	571	2.1718	0.0403	HOMO-1→LUMO+1	0.3857
				HOMO→LUMO	0.5890
	528	2.3494	0.0521	HOMO→LUMO+1	0.5741
	386	3.2079	0.6777	HOMO-1→LUMO+1	0.5060
4a	538	2.3033	0.0330	HOMO-1→LUMO	0.4241
				HOMO→LUMO+1	0.5626
	372	3.3308	1.3825	HOMO-1→LUMO	0.5549
				HOMO←LUMO+1	0.1066
4b	1158	1.0705	0	HOMO-2→LUMO	0.3939
				HOMO-1→LUMO+1	0.3810
4c	590	2.0992	0.0002	HOMO-2→LUMO+3	0.5160
	513	2.4153	0.0208	HOMO→LUMO	0.5407
4d	650	1.9057	0	HOMO→LUMO	0.6681
4e	531	2.3325	0.0344	HOMO→LUMO	0.4928
	404	3.0665	0.0586	HOMO-2→LUMO	0.4002
				HOMO-2→LUMO+1	0.5415
				HOMO-1→LUMO+1	0.1086

**E* (eV), Energy in electronvolt; *f*, oscillator force; *P*, probability.

J. Mex. Chem. Soc. **2025**, *69*(2)
Regular Issue

ISSN-e 2594-0317

References

1. Jung, S.-H.; Choi, J.-H.; Yang, S.-M.; Cho, W.-J.; Ha, C.-S. *Mater. Sci. Eng. B.* **2001**, *85*, 160–164. DOI: https://doi.org/https://doi.org/10.1016/S0921-5107(01)00600-6.
2. Taniguchi, M.; Lindsey, J. S.; Bocian, D. F.; Holten, D. *J. Photochem. Photobiol. C Photochem. Rev.* **2021**, *46*, 100401. DOI: https://doi.org/https://doi.org/10.1016/j.jphotochemrev.2020.100401.